

The CMB power spectrum at $\ell = 30 - 200$ from QMASK

Yongzhong Xu¹, Max Tegmark¹, Angelica de Oliveira-Costa¹

¹Dept. of Physics, Univ. of Pennsylvania, Philadelphia, PA 19104; xuyz@physics.upenn.edu

(April 26, 2024. To be submitted to Phys. Rev. D.)

We measure the cosmic microwave background (CMB) power spectrum on angular scales $\ell \sim 30 - 200$ from the QMASK map, which combines the data from the QMAP and Saskatoon experiments. Since the accuracy of recent measurements leftward of the first acoustic peak is limited by sample-variance, the large area of the QMASK map (648 square degrees) allows us to place among the sharpest constraints to date in this range (whose accuracy will not be surpassed until the day after tomorrow!), in good agreement with BOOMERanG and (on the largest scales) COBE/DMR. By band-pass-filtering the QMAP and Saskatoon maps, we are able to spatially compare them scale-by-scale to check for beam- and pointing-related systematic errors.

I. INTRODUCTION

After the discovery of large-scale Cosmic Microwave Background (CMB) fluctuations by the COBE satellite [1], experimental groups have forged ahead to probe ever smaller scales. Now that TOCO [2,3], Boomerang [4] and Maxima [5] have convincingly measured the location and height of the first acoustic peak, attention is shifting to still smaller scales to resolve outstanding theoretical questions. For instance, the question of whether the second peak is low as measured by Boomerang or high as reported by CBI [6] has important implications for the cosmic baryon density [7,8]. However, it remains important to improve measurements on larger angular scales as well, both for measuring cosmological parameters and to cross-validate different experiments against potential systematic errors. This is the goal of the present paper.

Since the accuracy of recent measurements leftward of the first acoustic peak is limited by sample-variance rather than instrumental noise, we will use the largest area CMB map available to date with degree scale angular resolution. This map, nicknamed QMASK [9], is shown in Figure 1 and combines the data from the QMAP [10–12] and Saskatoon [13–15] experiments into a 648 square degree map around the North Celestial Pole. This map has been extensively tested for systematic errors [9], with the conclusion that the QMAP and Saskatoon experiments agree well overall. However, for the present power spectrum analysis, it is important to perform additional systematic tests to see if there is evidence of scale-dependent problems in any of the maps. In particular, pointing problems, beam uncertainties, sampling and pixelization effects can smear the maps in a way that changes the shape of the power spectrum, suppressing small-scale fluctuations.

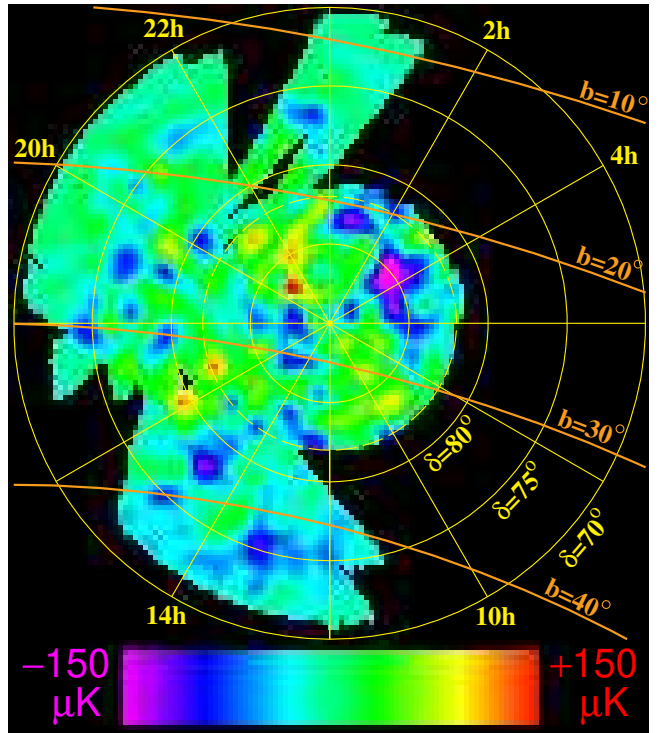


FIG. 1. Wiener-filtered QMASK map combining the QMAP and Saskatoon experiments. The CMB temperature is shown in coordinates where the north celestial pole is at the center of the dashed circle of 16° diameter, with R.A. being zero at the top and increasing clockwise. This map differs from the one published in [9] by the erasing of QMAP information for $\ell \gtrsim 200$ described in the text.

The rest of this paper is organized as follows. We perform a scale-by-scale comparison of QMAP and Saskatoon in Section II, finding good agreement but a hint of suppressed QMAP power for $\ell \gtrsim 200$. We present a technique for erasing this type of unreliable information, and apply it to produce a new combined QMASK map where all the statistical weight for $\ell \gg 200$ comes from Saskatoon. We compute the power spectrum of this combined map and summarize our conclusions in Section III.

II. A SCALE-BY-SCALE COMPARISON OF SASKATOON AND QMAP

In this section, we will compare the QMAP and Saskatoon data scale-by-scale, *i.e.*, in different multipole intervals. Based on the test results, we produce a new QMASK combination map giving zero statistical weight to QMAP signal for $\ell \gg 200$ to be conservative.

A. Method

Previous comparisons between CMB data sets have been done either spatially or in terms of power spectra (discarding phase information). Since two inconsistent maps can have identical power spectra, one should be able to obtain still stronger tests for systematic errors by comparing power *with* phase information. For instance, one could imagine band-pass filtering the two maps to retain only a particular range of multipoles ℓ , and then testing whether these two filtered maps were consistent. We will now describe a simpler way of implementing a test in this spirit.

Numerous map comparisons have been performed with the “null-buster” test [16]

$$\nu \equiv \frac{\mathbf{z}^t \mathbf{N}^{-1} \mathbf{S} \mathbf{N}^{-1} \mathbf{z} - \text{tr} \{ \mathbf{N}^{-1} \mathbf{S} \}}{[2 \text{tr} \{ \mathbf{N}^{-1} \mathbf{S} \mathbf{N}^{-1} \mathbf{S} \}]^{1/2}}, \quad (1)$$

where ν can be interpreted as the number of “sigmas” at which the difference map \mathbf{z} is inconsistent with pure noise. If the two maps are stored in vectors \mathbf{x}_1 and \mathbf{x}_2 and have noise covariance matrices \mathbf{N}_1 and \mathbf{N}_2 , then a weighted difference map $\mathbf{z} \equiv \mathbf{x}_1 - r\mathbf{x}_2$ will have noise covariance $\mathbf{N} \equiv \mathbf{N}_1 + r^2\mathbf{N}_2$. The matrix \mathbf{S} tells the test which modes (linear combinations of the pixels \mathbf{z}) to pay most attention to, and can be chosen arbitrarily. The choice $\mathbf{S} = \mathbf{N}$ gives a standard χ^2 -test. It can be shown [16] that the null hypothesis that \mathbf{z} is pure noise (that $\langle \mathbf{z} \mathbf{z}^t \rangle = \mathbf{N}$) is ruled out with maximal significance if \mathbf{S} is chosen to be the covariance of the expected signal in the map, *i.e.*, $\mathbf{S} = \langle \mathbf{z} \mathbf{z}^t \rangle - \mathbf{N}$. In our case, we choose \mathbf{S} to be the CMB covariance matrix corresponding to a power spectrum

$$\delta T_\ell = \begin{cases} 1 \mu\text{K} & \text{if } \ell \in [\ell_{\min}, \ell_{\max}]; \\ 0 \mu\text{K} & \text{otherwise.} \end{cases}, \quad (2)$$

ensuring that the test only uses information in the multipole interval $[\ell_{\min}, \ell_{\max}]$. The overall normalization of \mathbf{S} is irrelevant, since it cancels out in equation (1).

B. Test results

The QMASK map was shown to be inconsistent with noise at the 62σ level [9]. In the region where the QMAP and Saskatoon maps overlap, they were found to detect

signal at 40σ and 21σ , respectively, while the difference map was consistent with pure noise. Which angular scales are contributing most of this information, and how well do the two maps agree scale-by-scale?

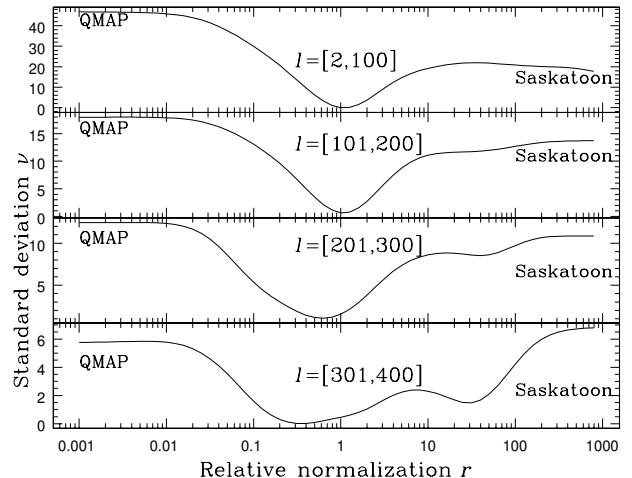


FIG. 2. Comparison of the QMAP and Saskatoon experiments on different angular scales, corresponding to the multipole ranges shown in square brackets. The curves show the number of standard deviations (“sigmas”) at which the difference map $\tilde{\mathbf{x}}_{\text{QMAP}} - r\tilde{\mathbf{x}}_{\text{SASK}}$ is inconsistent with mere noise. Note that this is only for the spatial region observed by both experiments.

To answer these questions, Figure 2 shows the result of comparing QMAP with Saskatoon in the four multipole intervals $[2, 100]$, $[101, 200]$, $[201, 300]$, and $[301, 400]$. QMAP is seen to detect signal in the overlap region at 47σ , 18σ , 12σ and 6σ , respectively, whereas the corresponding numbers for Saskatoon are 18σ , 14σ , 11σ and 7σ . In other words, QMAP dominates on large scales, whereas Saskatoon has an edge on small scales because of superior angular resolution.

Although QMAP and Saskatoon both detect significant CMB signal in all four bands, this signal is seen to be common to both maps since the difference maps \mathbf{z} for $r = 1$ are consistent with noise. Furthermore, there is no evidence of relative calibration errors for the $[2, 100]$ or $[101, 200]$ bands, since the minima of these two curves are at $r \approx 1$. However, the situation is less clear on smaller scales: the best-fit amplitude of QMAP is only 63% of the amplitude of Saskatoon for $\ell \in [201, 300]$, and even lower for $\ell \in [301, 400]$. None of these departures of the minimum from $r = 1$ are statistically significant — we cannot determine whether this is a problem or not simply because the amount of information in the maps drops sharply on small scales where detector noise and beam dilution become important. However, whereas the Saskatoon information was extracted from highly oversampled calculations of the relevant beam patterns on the sky, and should be reliable on small scales, there are a number of reasons why the QMAP data may only be valid on larger ($\ell \lesssim 200$) angular scales [10–12]:

1. The QMAP pointing solution was only accurate to this level [11], and small residual pointing uncertainties could have effectively smoothed the map, suppressing power for $\ell \gg 200$ relative to Saskatoon just as Figure 2 indicates.
2. The QMAP maps were generated by subdividing the sky into square pixels of side $\theta = 0.3125^\circ$, and the effect of this pixelization may well become important on angular scales substantially exceeding $\ell \sim 1/\theta \approx 200$, suppressing power on these scales.
3. Flight 1 of QMAP [10], which dominates the sky coverage in Figure 1 was sampled at a relatively low rate, causing the effective beam shapes to be elongated along the scan direction. Since this ellipticity was not modeled in the mapmaking algorithm [12], the resulting smoothing would again be expected to suppress power on scales $\ell \gg 200$.

C. Erasing the small-scale information from QMAP

Since it is possible that the $\ell \gtrsim 200$ power in QMAP has too low an amplitude for the above-mentioned reasons, let us erase this information as a precaution, to be conservative. By this we do not mean removing the *signal* (smoothing the map), which would just lead to further underestimation of the true power. Rather, we mean removing the *information*, *i.e.*, doing something that causes subsequent analysis steps (like combining with Saskatoon or measuring the power spectrum) to give negligible statistical weight to the small-scale QMAP signal. We achieve this by creating a random map with very large small-scale noise and adding it to the QMAP map, modifying its noise covariance matrix \mathbf{N} accordingly.

In practice, we start by generating a white noise map $\mathbf{x}_{\text{white}}$ which has the following properties: it covers the same sky region as QMAP, and each pixel temperature is drawn independently from a Gaussian distribution with zero mean and standard deviation σ , giving it a noise covariance matrix $\Sigma_{\text{white}} = \sigma^2 \mathbf{I}$. This makes its angular power spectrum C_ℓ independent of ℓ . We then apply the Laplace operator ∇^2 to the mock map. Since it is pixelized on a square grid, we do this in practice by multiplying by a matrix \mathbf{L} that subtracts each pixel from the average of its four nearest neighbors. The transformed map $\mathbf{x}_{\text{blue}} = \mathbf{L}\mathbf{x}_{\text{white}}$ thereby obtains a very blue power spectrum $C_\ell \propto \ell^4$, since Laplace transformation corresponds to multiplying by $\ell(\ell+1)$ in the Fourier (multipole) domain. We choose the normalization factor σ such that the blue noise starts dominating the noise and signal of the QMAP map around $\ell \sim 200$. Since the CMB power falls off as $C_\ell \propto \ell^{-2}$, the result is that the added noise is negligible for $\ell \ll 200$ and dominates completely for $\ell \gg 300$. Finally, we add this blue noise map to the QMAP map, obtaining

$$\mathbf{x}_{\text{new}} = \mathbf{x}_{\text{QMAP}} + \mathbf{x}_{\text{blue}} = \mathbf{x}_{\text{QMAP}} + \mathbf{L}\mathbf{x}_{\text{white}}, \quad (3)$$

$$\Sigma_{\text{new}} = \Sigma_{\text{QMAP}} + \Sigma_{\text{blue}} = \Sigma_{\text{QMAP}} + \sigma^2 \mathbf{L}\mathbf{L}^t. \quad (4)$$

We then combine this new map with the Saskatoon data as in [9]. The result is shown in Figure 1, and looks almost unchanged since Wiener filtering suppresses noisy modes and the smallest scales were noisy to start with.

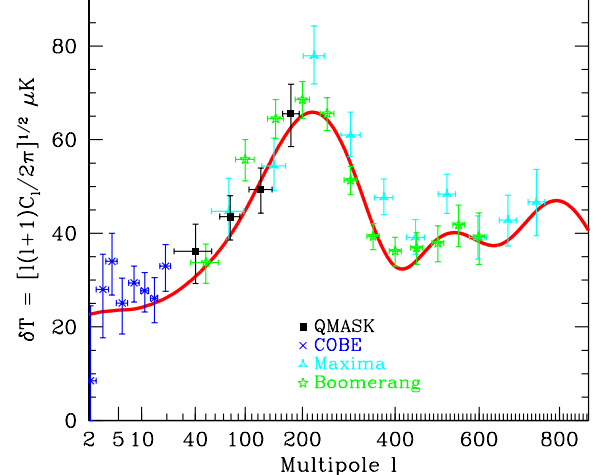


FIG. 3. Angular power spectrum $\delta T \equiv [\ell(\ell+1)C_\ell/2\pi]^{1/2}$ of CMB anisotropy from the combined QMASK data. For comparison, we also plot the a recent “concordance” model [17] and the power the measurements from COBE/DMR, MAXIMA and BOOMERanG.

ℓ	$\delta T_\ell^2 [\mu K^2]$
40 ± 16	1308 ± 452
79 ± 13	1899 ± 410
125 ± 19	2436 ± 471
178 ± 15	4265 ± 869

Table 1. The power spectrum $\delta T \equiv [\ell(\ell+1)C_\ell/2\pi]^{1/2}$ from the QMASK map. The tabulated error bars are uncorrelated between the four measurements, but do not include an overall calibration uncertainty of 10% for δT .

III. THE ANGULAR POWER SPECTRUM

In this section, we compute the angular power spectrum of the QMASK map produced in the previous section, shown in Figure 1. It contains 6495 pixels and covers a 648 square degree sky region. We calculate the angular power spectrum using the quadratic estimator method of [18,19], implemented as described in [20,21]. This method involves the following steps: (i) S/N compression of data and relevant matrices by omitting Karhunen-Loève (KL) eigenmodes with very low signal-to-noise ratio, (ii) computation of Fisher matrix and raw quadratic estimators, (iii) decorrelation of data points. We compute the power in 20 bands from $\ell = 2$ to 400 of width $\Delta\ell = 20$, which takes about a week on a workstation. We then average these rather noisy measurements

into six (still uncorrelated) measurements. The first four probe angular scales where the above-mentioned QMAP systematics are likely to be negligible, incorporating the first 9 ℓ -bands (up to $\ell = 180$), and are shown in Figure 3 and listed in Table 1. The vertical bars show the mean and rms width of the corresponding window functions.

Figure 3 shows that our results agree well with the “concordance” model of [17]. They are also consistent with BOOMERanG [4] and Maxima [5] once calibration uncertainties are taken into account. The QMAP and Saskatoon calibration uncertainties are 6% – 10% and 10% after correcting the original δT results [10,14] by a factor 1.05 using the latest Cassiopeia A data [22] as in [23]. Although the uncorrelated components of this may average down somewhat when the two maps are combined, we quote a 10% uncertainty on our result to be conservative. Our results are also consistent with those obtained from QMAP and Saskatoon alone. Our leftmost data point agrees well with the last point measured from COBE/DMR [24] by [18].

The BOOMERanG power spectrum was based on a map area of 436 square degrees [4], so one might expect our error bars on large scales to be a factor $(648/436)^{1/2} \approx 1.2$ smaller. Our actual error bars on δT_ℓ^2 are only about 10% smaller than those from BOOMERanG on the best QMASK scales after adjusting for bandwidth differences, which is because of BOOMERanG’s lower noise levels (the scan strategy and $1/f$ -noise of QMAP introduced a non-negligible amount of noise even on the largest scales). We note that the substantial reduction in error bars relative to the original Saskatoon analysis [14] is due to additional information not only from QMAP, but from Saskatoon as well. This is because our present method extracts all the information present, whereas that employed in [14] was limited to information along radial scans, not using phase information between scans.

Our last two measurements are $\delta T_\ell^2 = (4265 \pm 726) \mu\text{K}^2$ at $\ell = 259 \pm 46$ and $\delta T_\ell^2 = (2596 \pm 1795) \mu\text{K}^2$ at $\ell = 335 \pm 58$. The first of these points is significantly below both the original Saskatoon analysis [14] and our own power spectrum measurement of the Saskatoon-only map (including non-radial information), showing that QMAP is still contributing substantially even at $\ell \sim 250$, on scales where the above-mentioned systematics are likely to be important. This means that these two points should not be used for cosmological parameter fitting.

The foreground contamination has been previously quantified for both Saskatoon [25] and QMAP [26], and is estimated to contribute at most a few percent to the angular power spectrum reported here. The errors reported on the power spectrum assume that the underlying CMB signal is Gaussian, which is supported by a recent Gaussianity analysis of the QMASK map [27].

In conclusion, we have measured the CMB power spectrum on angular scales $\ell \sim 30 – 200$ from the QMASK map, placing among sharpest constraints to date on the

shape of the CMB power spectrum as it rises towards the first acoustic peak. Our window functions, the combined map and its noise covariance matrix are available at www.hep.upenn.edu/~xuyz/qmask.html.

The authors wish to thank Mark Devlin and Lyman Page for useful comments. Support for this work was provided by NSF grant AST00-71213, NASA grant NAG5-9194, the University of Pennsylvania Research Foundation, and the Zaccheus Daniel Foundation.

- [1] G. F. Smoot *et al.*, ApJ **396**, L1 (1992).
- [2] E. Torbet *et al.*, ApJL **521**, L79 (1999).
- [3] A. D. Miller *et al.*, ApJL **524**, L1 (1999).
- [4] P. de Bernardis *et al.*, Nature **404**, 955 (2000).
- [5] S. Hanany *et al.*, ApJL **545**, L5 (2000).
- [6] S. Padin *et al.*, ApJL **549**, L1 (2001).
- [7] M. Tegmark and M. Zaldarriaga, Phys. Rev. Lett. **85**, 2240 (2000).
- [8] A. E. Lange *et al.*, astro-ph/0005004 (2000).
- [9] Y. Xu, M. Tegmark, A. de Oliveira-Costa, M. Devlin, T. Herbig, A. D. Miller, C. B. Netterfield, and L. A. Page 2001, astro-ph/0010552, *Phys. Rev. D*, in press.
- [10] M. Devlin, A. de Oliveira-Costa, T. Herbig, A. D. Miller, C. B. Netterfield, L. A. Page, and M. Tegmark, ApJL **509**, L77 (1998).
- [11] T. Herbig *et al.*, ApJL **509**, L73 (1998).
- [12] A. de Oliveira-Costa, M. Devlin, T. Herbig, A. D. Miller, C. B. Netterfield, L. A. Page, and M. Tegmark, ApJL **509**, L77 (1998).
- [13] C. B. Netterfield *et al.*, ApJ **445**, L69 (1995).
- [14] C. B. Netterfield, M. J. Devlin, N. Jarosik, L. A. Page, and E. J. Wollack; ApJ, **474**, 47 (1997)
- [15] M. Tegmark *et al.*, ApJL **474**, L77 (1996a).
- [16] M. Tegmark, ApJ **519**, 513 (1999).
- [17] M. Tegmark, M. Zaldarriaga, and A. J. S. Hamilton, Phys. Rev. D **63**, 043007 (2001).
- [18] M. Tegmark, Phys. Rev. D **55**, 5895 (1997).
- [19] J. R. Bond, A. H. Jaffe, and L. E. Knox, ApJ **533**, 19 (2000).
- [20] N. Padmanabhan, M. Tegmark, and A. J. S. Hamilton, astro-ph/9911421, *ApJ*, in press.
- [21] M. Tegmark and A. de Oliveira-Costa, astro-ph/0012120 (2000).
- [22] B. Mason *et al.*, Astron. J **118**, 2908 (1999).
- [23] E. Gawiser and J. Silk, Phys. Rep. **333**, 245 (2000).
- [24] C. L. Bennett *et al.*, ApJ **464**, L1 (1996).
- [25] A. de Oliveira-Costa, A. Kogut, M. J. Devlin, C. B. Netterfield, L. A. Page, E. J. Wollack, ApJ **482**, L17 (1997).
- [26] A. de Oliveira-Costa, M. Tegmark, M. J. Devlin, L. M. Haffner Haffner, T. Herbig, A. D. Miller, L. A. Page, R. J. Reynolds, S. L. Tufts, ApJL **542**, L5 (2000).
- [27] C. G. Park, C. Park, B. Ratra, and M. Tegmark 2001, astro-ph/0102406, *ApJ*, in press.